Science Press

ARTICLE

Preparation and Electrochemical Performance Characterization of Si/Graphite/Disordered-Carbon Composite Anode for Lithium-Ion Batteries

Li Tao[1,2],   Li Meng[2],   Li Na[1],   Wang Changhua[1],   Zhu Dongxia[3],   Zhang Lijiu[1],   Li Shengchen[1],   Deng Nan[1]

[1] Guobiao (Beijing) Testing & Certification Co., Ltd, Beijing 101400, China; [2] Grinm Group Corporation Limited, Beijing 100088, China; [3] Shanghai Nonferrous Metals Industry Technology Monitoring Center Co., Ltd, Shanghai 200431, China

Abstract: An optimized structure of the Si/graphite/disorded-carbon (Si/G/DC) composites was proposed and prepared to improve the cycling performance by ultra-fine grinding of elemental mixtures of nano-silicon, graphite and sucrose followed by thermal treatment. The morphology, electrochemical performance, cycling stability and optimization of silicon content of Si/G/DC composites were investigated. Results show that the use of nano-silicon materials loaded on graphite carbon matrix can effectively improve the electrochemical performance of anode materials combined with high-temperature pyrolysis technology. With graphite as buffer matrix and conductive network and amorphous carbon coating, the Si/G/DC composite shows excellent electrochemical performance. The amorphous carbon coating in the Si/G/DC composite can apparently reduce the possibility of contact loss between silicon and electrolyte, and help to maintain the mechanical stability by relieving stresses resulting from silicon volume change.

Key words: lithium-ion battery; silicon; Si/graphite/disorded-carbon composite; anode

The rapid volume change in the process of lithium intercalation and extraction inevitably leads to the cracking or fragmentation of anode materials and results in the capacity loss in the cycle, which hinders the commercial application of silicon anode materials[1-5]. In order to improve the stability of silicon-based anodes, silicon/carbon composite anodes have attracted extensive attention due to their softness, relatively low mass, compliance, excellent electronic conductivity, reasonable lithium intercalation performance, small volume expansion and stress buffering properties of carbon materials[6-9]. In recent years, silicon/carbon composites have been synthesized by silicon and carbon with different particle sizes and crystal forms, including nano-crystalline and amorphous silicon, graphite, meso-scale carbon microbeads (MCMB) and disordered carbon[7,10-21].

There are many ways to prepare silicon/carbon composite anodes, which can be classified into six types based on their preparation procedure: (1) ball or mechanical milling, (2) chemical/thermal vapor deposition (CVD/TVD), (3) pyrolysis, (4) combination of pyrolysis/CVD/TVD and mechanical milling, (5) chemical reaction of gels, (6) other methods[22-30]. In order to overcome Si pulverization during cycling, Hsu[31] proposed a double core-shell carbon/silicon/graphite composite anode using high-purity silicon powder with MCMB and amorphous pitch to stabilize the structure of silicon, and the prepared composites show high reversible capacity and good cycle stability. MCMB was used as the core material, and the reversible capacity was increased by adding high-purity silicon powder on its surface[31]. The pitch coating as the shell was prepared by high temperature carbonization process[31]. Ryu[15] reported a kind of mixed silicon carbon composite anode at molecular level. Through the pyrolysis of silane and subsequent mechanical grinding, the disordered silicon carbon bonds are dissociated and re-aggregated by electrochemistry during the cycle.

Here we proposed and prepared an optimized structure of

the Si/graphite/disordered-carbon(Si/G/DC) composites to improve the cycling performance by ultra-fine grinding of elemental mixtures of nano-silicon, graphite and sucrose followed by thermal treatment. The use of nano silicon materials loaded on graphite carbon matrix can effectively improve the electrochemical performance of anode materials, and combined with high-temperature pyrolysis technology, organic carbon source carbon was pyrolyzed to coat nano-silicon powder. The synthetic graphite (AGP-8) which is commonly used in lithium-ion batteries industry field as graphite material was used as graphite carbon matrix, which can effectively improve the cycle stability and meet the requirements for industrial production. And owing to the simplicity of ultra-fine grinding method, it is believed that this method is easy to scale up and will lead to an industrial route for the mass production of silicon-based anode materials. There are many kinds of carbohydrate organic carbon sources, such as glucose, sucrose, fructose, cellulose and starch. Generally speaking, using sucrose as organic carbon source is a very common method to protect materials for its cheapness. The Si/graphite (Si/G) composites without disorded-carbon coating were also synthesized using ultra-fine grinding method. The morphology, electrochemical performance, cycling stability and optimization of silicon content of Si/G/DC and Si/G composites were investigated.

1 Experiment

1.1 Materials synthesis

The synthetic process of the material can be divided into two parts: ultrafine grinding and spray drying. Ultrafine grinding mainly plays the role of abrasive materials, and spray drying plays a role in compound granulation besides drying slurry. The key step for the preparation of silicon carbon composites is the dispersion of nano-silicon powder and the composite of silicon and carbon. In this experiment, a ultra-fine grinding equipment with the functions of grinding, stirring and dispersing was selected. The motor drives the agitator in the grinding cylinder to rotate through the variable speed device. Under the agitation of the agitator, the grinding medium and material make multi-dimensional circular motion and rotation motion, producing continuous intense motion of up and down, left and right displacement in the grinding cylinder. The extruding force produced from gravity of grinding medium and spiral rotation rubs makes the material comminuted under the action of spiral rotation rubs, impacts and shears. In this experiment, two steps of ultrafine grinding were used. The first step was to disperse nano-silicon particles, and the second step was to promote the combination of silicon and carbon through the shear action of ultrafine grinding.

1.1.1 Preparation of Si/G/DC composite

Fig. 1a shows the preparation process of Si/G/DC composite. Mixtures of elemental powders of nano-Si powders (with mean particle size of 20~70 nm, from Institute of Metal Research, Chinese Academy of Sciences), synthetic
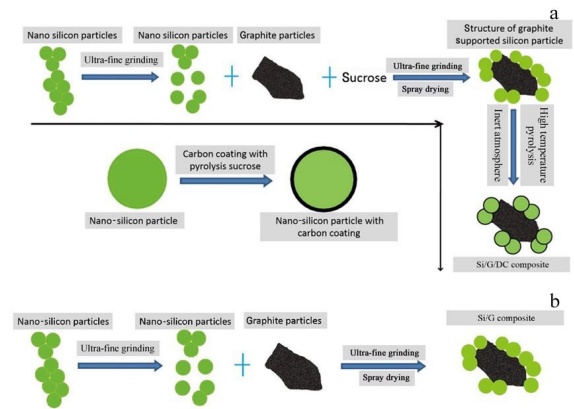

Fig.1 Preparation process of Si/G/DC (a) and Si/G (b) composites

graphite (AGP-8, 3~15 μm, BTR Battery Materials Co., Ltd) and sucrose ($C_{12}H_{22}O_{11}$, analytically pure, Sinopharm Chemical Reagent Beijing Co., Ltd, the yield of amorphous carbon is 40%) with elemental composition of [4.644wt% Si]-[88.236wt% C] - [7.12wt% sucrose] were used for the preparation of the Si/G/DC composite. At first, the nano-Si powders were dispersed in alcohol using ultra-fine grinding for 1 h to form silicon slurry, and then the graphite and sucrose were subjected to the prepared silicon slurry with ultra-fine grinding for 2 h to form a homogeneous solution. The precursor was obtained with spray drying the mixture solution. The spray-dried precursor was calcined at 650 °C for 10 h in ultra-high purity argon with heating rate of 5 K/min and flow rate of 50 mL/min, and then cooled naturally to ambient temperature. The composite material was further ground by planetary ball milling and sieved by 300 mesh sieve. The final substance was the Si/G/DC composite. The contents of silicon were optimized onto the graphite carbon matrix with the elemental composition of [18.576wt% Si] - [74.304wt% C] - [7.12wt% sucrose] and [37.152wt% Si] - [55.728wt% C]-[7.12wt% sucrose].

1.1.2 Preparation of the Si/G composite

Fig. 1b shows the preparation process of Si/G composite. Mixtures of elemental powders of nano-Si powders and synthetic graphite (AGP-8) with elemental composition of [5wt% Si] - [95wt% C] were subjected to prepare the Si/G composite. Nano-Si powders were first dispersed in alcohol using ultra-fine grinding for 1 h to form silicon slurry, and then the graphite was subjected to silicon slurry with ultra-fine grinding for 2 h to form a homogeneous solution. The Si/G composite was obtained by spray drying the above solution. The composite material was further ground by planetary ball milling and sieved by 300 mesh sieve (50 μm). The final substance was the Si/G composite.

1.2 Materials characterization

The composites were characterized using X-ray diffractometer (XRD, Philip X Pert-MPD) with Cu-Kα ($\lambda = 0.154\ 06$ nm) radiation for qualitative phase analysis. The scanning electron microscope (SEM, Hitachi S4800) was used to study the microstructure and morphology of composites and electrodes. Transmission electron microscope (TEM) and

selected area electron diffraction (SAED) were taken on JEOL JEM-2010 with the acceleration voltage of 200 kV and point resolution of 0.19 nm. Brunauer-Emmett-Teller specific surface area analyzer (Micromeritics Tristar 3000) was used to measure the specific surface area.

The electrode was prepared on copper substrate to evaluate the electrochemical characteristics, using Super P carbon black (CB, TIMCAL) as conductive additive and Poly-vinylidene-fluoride (PVDF) as binder, with 80% composite, 10% Super P and 10% PVDF binder composition.

Coin cells (CR2032) were used with Li as counter electrode, porous polypropylene (celgard 2300) as separator, 1.0 mol/L $LiPF_6$ in a mixture of DMC, DEC and EC (1:1:1 in volume) as electrolyte. Cycling tests were performed at 0.005~2.0 V with 50 mA/g constant current using LAND CT2001A battery cycler. The cells were carefully disassembled after cycling, and the electrodes were rinsed in dimethylcarbonate (DMC) solvent to remove residual electrolyte and dried in vacuum atmosphere for characterization.

2 Results and Discussion

Fig.2a and Fig.2b show the SEM and TEM images of nano-silicon particles. The nano-silicon particles are spherical with average diameter of 50~70 nm. Most of the particles agglomerate with each other, and a few particles with a diameter of 20 or 60 nm are isolated and dispersed. Most of the particles are connected by 3~5 spherical particles with diameter of 50~70 nm to form chain shape. Fig.2c and Fig.2d show the SEM images of graphite AGP-8. The AGP-8 graphite material is a kind of natural graphite which is pelletized by composite and mainly used for the negative material of lithium-ion battery, with D_{50} between 10~14 μm, specific surface area between 2.5~4.0 m^2/g, and tap density is 0.8557 g/cm^3. From Fig.2c, the AGP-8 graphite materials are mainly composed of spherical particles with 3~15 μm in diameter and a small amount of irregular particles with 5~15 μm in diameter . As shown in Fig.2d, the spherical particles and single irregular particles are all composed of lamellar particles, with clear particle boundary.

Fig. 3a and 3b show the SEM images of nano-silicon material after ultrafine grinding and spray drying alone, which is mainly composed of spherical particles with 2~8 μm in diameter, and the surface is composed of a large number of 50~70 nm spherical silicon particles. Due to spray drying granulation, the nano-crystalline silicon particles are agglomerated to form heterogeneous silicon clusters. Fig. 3c and 3d are the SEM images of AGP-8 graphite after ultrafine grinding and spray drying alone, and the AGP-8 graphite changes to 3~25 μm flake particles after ultrafine grinding spray drying. For AGP-8 carbon materials, due to the spherical structure formed by natural graphite composite granulation, the composite structure of the material is destroyed during ultrafine grinding process. The spherical particles of 3~15 μm were ground into sheet particles, but the granulation effect of subsequent spray drying on the newly formed flake particles is not obvious. Fig.3e is the SEM image of Si/G composite. The Si/G composites are composed of flaky particles ranging from 5~30 μm with irregularly-shaped pattern, including ribbon, diamond and square. Compared with the AGP-8 graphite materials without any treatment shown in Fig.2c, the initial 3~15 μm spherical shaped graphite is ground to 5~30 μm irregular particles during the ultra-fine grinding process. The increase of particle size is mainly caused by spray granulation after ultrafine grinding. From Fig.3f, the magnified SEM image of the Si/G composite, the nano-Si particles are normally distributed in the graphite matrix. Fig.3g shows the SEM image of Si/G/DC composites. Similar to the Si/G composites, the Si/G/DC composites are
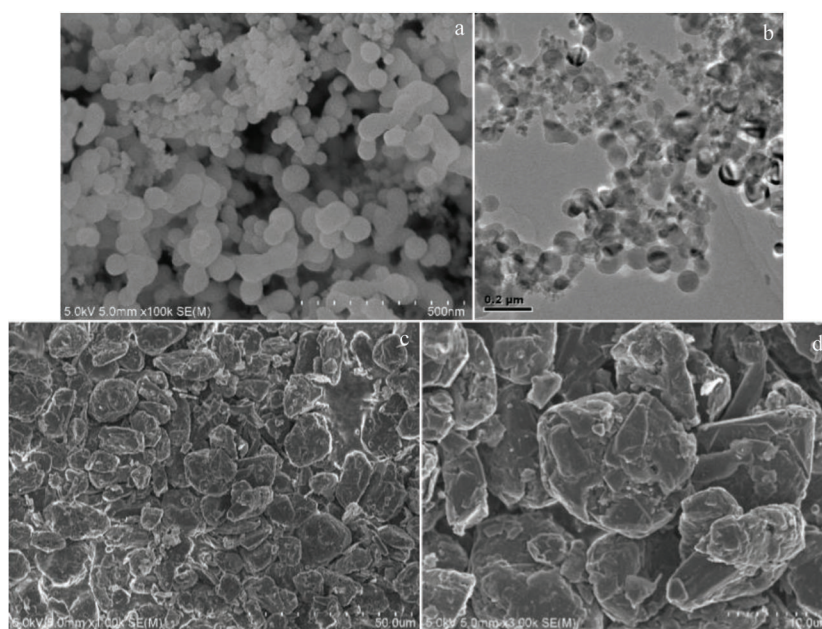

Fig.2　SEM (a) and TEM (b) images of nano-silicon particles; SEM images of graphite AGP-8 (c, d)
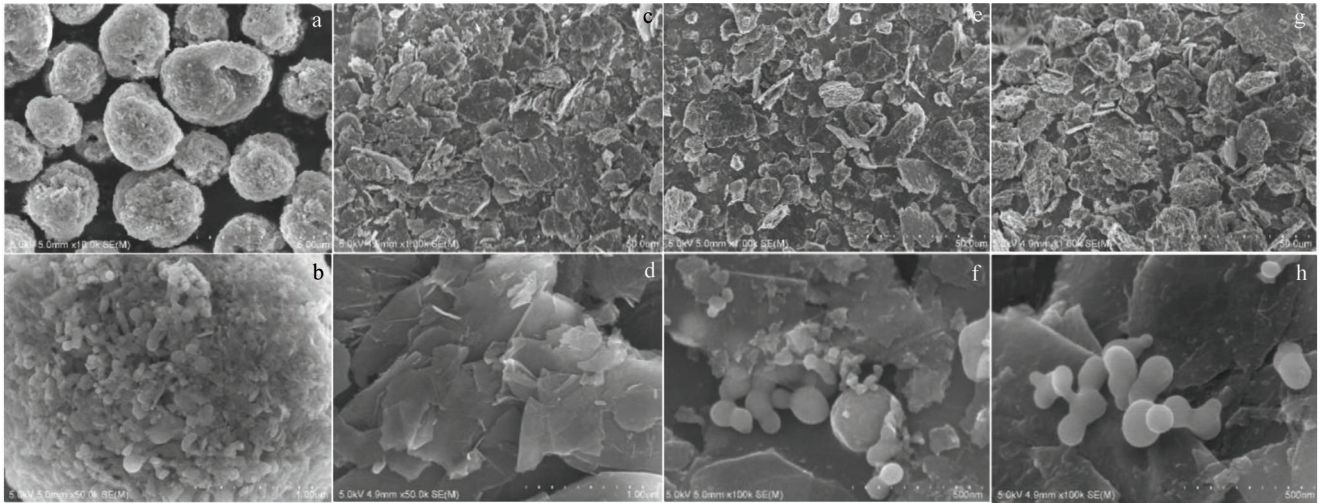
Fig.3　SEM images of nano-silicon (a, b) and AGP-8 graphite (c, d) after ultra-fine grinding; SEM images of the Si/G composite (e, f) and Si/G/DC composite (g, h)

also composed of irregularly-shaped flaky particles ranging from 5~30 μm. From Fig. 3h, spherical silicon particles with 50~70 nm in diameter are linked in chains and loaded on the surface of carbon particles. The Si/G/DC composite exhibits a specific surface area of 4.6 m²/g, higher than that of Si/G composite (4.2 m²/g), while the tap density of Si/G/DC and Si/G composite is 1.005 and 1.071 g/cm³, respectively. The grain sizes of Si/G and Si/G/DC composite are slightly larger than that of AGP-8 graphite after ultrafine grinding and spray

drying alone, which is mainly caused by the decrease of grinding effect caused by the addition of silicon material in ultrafine grinding.

The TEM observation in Fig. 4a and 4b shows that the spherical nano-silicon particles with 50~70 nm in average particle size are attached to the surface of graphite matrix, and there are amorphous carbon from sucrose coating on the silicon particles and filling among the silicon particles. The comparison of TEM images of initial nano-Si particle and the
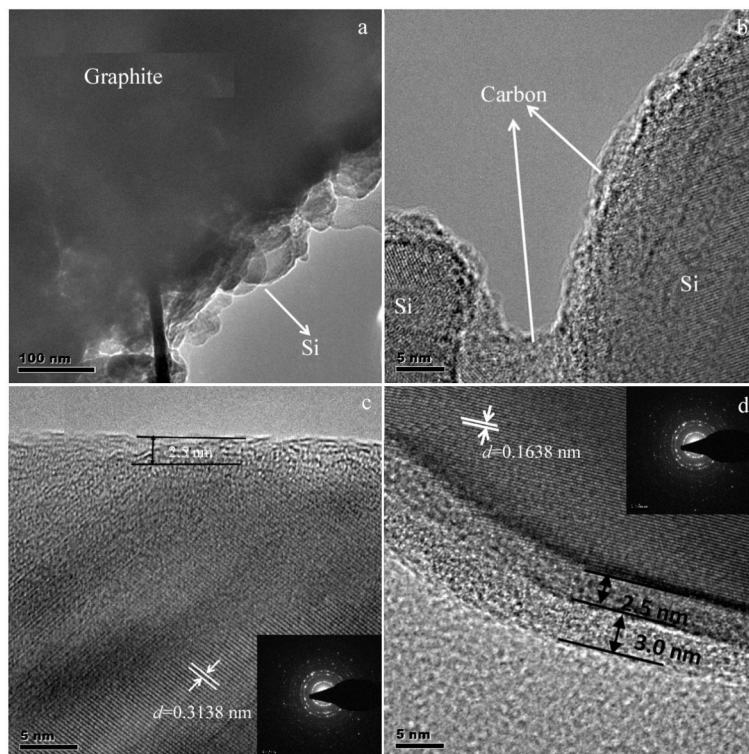

Fig.4　TEM images of Si/G/DC composite particle (a, b); TEM images and SAED patterns of initial silicon particle (c), silicon particle in Si/G/DC composite (d)

silicon particle in the Si/G/DC composite was used to explore the carbon coating silicon structure. From TEM image and SAED pattern of intial silicon particle in Fig.4c, it can be seen that there are lattice fringes formed by the nano-Si atomic ordering along the [111] direction with d(A)= 0.3138 nm. An amorphous passivation film with a thickness of 2~3 nm is coated on the surface of the crystal nano-silicon particle. Compared with the initial silicon particle in Fig.4c, there is a homogeneous amorphous carbon layer with thickness of 2~3 nm outside the oxide film of the silicon particle which is formed by the pyrolysis of sucrose observed in silicon particle in Si/G/DC composite as shown in Fig.4d. The experimental results are similar to research of Ng[32] who studied amorphous carbon-coated silicon nano-composites. The Si/G/DC composite structure can be confirmed: the nano-silicon particles with homogeneous amorphous carbon layer are loaded on the surface of graphite particles with conductive carbon network between particles. The graphite matrix can buffer the destroy of electrode structure due to the volume expansion of silicon particles. The pyrolytic carbon coating can further improve the conductivity of the composite material and silicon particles.

Fig. 5 gives the charge capacity and efficiency of nano-silicon, Si/G and Si/G/DC composite electrode using Super P carbon black as conductive additive. The first charge capacity of nano-silicon material is 2553 mAh/g, and the charge-discharge efficiency is 71%. The first charge capacity of Si/G composites is 487 mAh/g, and the charge-discharge efficiency is 73%. In addition, the first charge capacity of Si/G/DC composites is 535 mAh/g, and the charge-discharge efficiency is 81%. The reversible charge capacity of nano-silicon material is 708 mAh/g and the capacity retention is 28% at the 20th cycle. The reversible charge capacity of Si/G composite is 414 mAh/g and the capacity retention is 85% at the 20th cycle. The reversible charge capacity of Si/G/DC composite is 491 mAh/g and the capacity retention is 92% at the 20th cycle. The reversible charge capacity of Si/G/DC composite is 480 mAh/g and the capacity retention is 89% at the 100th cycle. Using graphite as buffer matrix and conductive network, the Si/G and Si/G/DC composite all show excellent electrochemical performance compared to the pure nano-
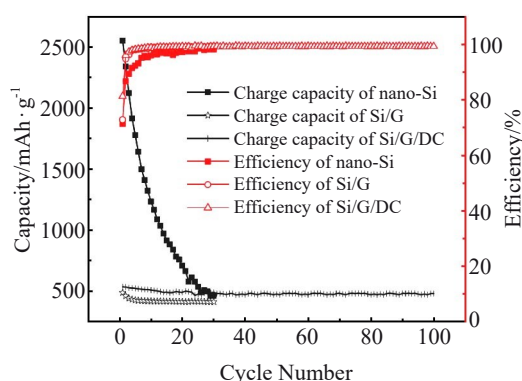

Fig.5   Charge capacity and efficiency of nano-silicon, Si/G and Si/G/DC composites electrode (80 mA/g)

silicon material, and the Si/G/DC composites have better electrochemical properties compared to Si/G composites.

As mentioned above, the Si/G and Si/G/DC composites have similar "silicon loaded on the graphite" structure, except that there are amorphous carbon from sucrose coating on the silicon particles and filling among the silicon particles for the Si/G/DC composite; meanwhile the amorphous carbon coated Si/G/DC composites can significantly reduce the possibility of contact loss between silicon and electrolyte. The comparison of electrochemical properties between Si/G composites and Si/G/DC composites clearly shows that the amorphous carbon coating has a positive and effective effect on the electrochemical properties of composites. The amorphous carbon coating in Si/G/DC composites with many nano-silicon particles adhered to the amorphous carbon has good porosity, and there are voids between particles which improve the capacity retention of Si/G/DC composites. The electrochemical reaction between electrolyte and silicon will lead to the volume change of silicon and separation of conductive path between silicon and other particles, resulting in the loss of active substances. The amorphous carbon coated Si/G/DC composite structure can also maintain mechanical stability by eliminating the stress caused by the volume change of silicon. Therefore, the Si/G/DC composites show better electrochemical performance compared to the Si/G composites.

Fig.6 shows the surface and cross section SEM micrographs of Si/G/DC composite electrode before and after 40 cycles. Compared with the electrode before cycling (Fig.6a and 6c), the SEM images after cycling (Fig.6b and 6d) show that the electrode of Si/G/DC composite has no microstructure failure or crack even after 40 cycles. For the homogeneous distribution of Si within the graphite matrix during ultra-fine grinding, Si/G/DC composite shows good microstructure stability, electrode structural integrity during the alloying and de-alloying process, and then good capacity retention ability. Moreover, the amorphous carbon coated Si/G/DC composite structure can also help to maintain structural stability of the electrode and improve the mechanical properties of the composites by strengthening the adhesion between Si and graphite. As shown in Fig.6e and 6f, the cross section SEM micrograph of Si/G/DC composite electrode before and after cycling is used to study the structural stability of the electrode and the material deterioration during repeated electrochemical reaction. The thickness of the electrode after cycling remains 75 μm and the electrode becomes more compact compared with the electrode before cycling. Meanwhile, the contact of the electrode material and the copper substrate remains well. This may be the main reason why Si/G/DC composites show better electrochemical properties than Si/G composites.

In order to study the relationship between the capacity and the Si contents of the composite, the content of silicon was optimized onto the graphite carbon matrix. The elemental composition [37.152wt% Si] - [55.728wt% C] - [7.12wt% sucrose] (marked as A), [18.576wt% Si] - [74.304wt% C] - [7.12wt% sucrose] (marked as B) and [4.644wt% Si] -
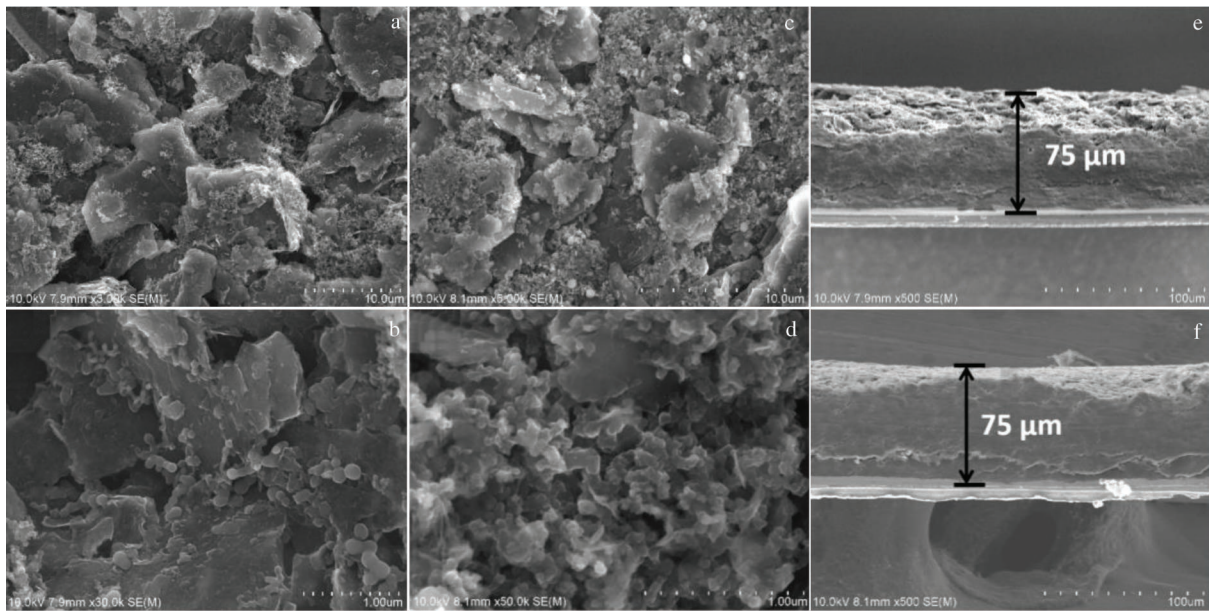
Fig.6　SEM images of surface (a~d) and cross section (e, f) of Si/G/DC electrode: (a, c, e) before 40 cycles and (b, d, f) after 40 cycles

[88.236wt% C]-[7.12wt% sucrose] (as studied above, marked as C) were used to prepare the Si/G/DC composite.

As shown in Fig.7a, sample A mainly consists of spherical particles with 2~5 μm in diameter. It can be seen from the enlarged image of a single spherical particle in Fig.7b that the particle surface is composed of 50~70 nm spherical silicon particles. The spherical particles are agglomerated spheres composed of nano-silicon particles, and the ground carbon material is also mixed among the nano-silicon particles on the agglomerated sphere surface. As shown in Fig.7c, sample B mainly consists of 5~30 μm flake particles and spherical particles with 2~5 μm in diameter. The shape of flake particles is irregular, and the morphology of spherical particles is similar to that of agglomerated silicon balls in sample A. The spherical particles in sample B are also agglomerated silicon balls, but the number of agglomerated silicon balls is

significantly reduced. As can be seen from the enlarged image of flake carbon particles in Fig.7d, a large number of 50~70 nm spherical silicon particles are loaded on the particle surface, and the agglomeration of silicon particles is obvious.

Fig.7e shows the charge capacity and efficiency of Si/G/DC composites with different Si contents. The first lithium charge capacities of the sample A, B, C are 1053, 770 and 535 mAh/g, respectively. According to the calculation of 360 mAh/g lithium discharge capacity of carbon in the composite, the specific lithium discharge capacities of silicon for the sample A, B, C are 2093, 2410 and 3860 mAh/g, respectively. Because the silicon in sample A and B exists in the form of agglomerated silicon spheres, the specific capacity of lithium removal of silicon is lower than that of single nano-silicon. The silicon in sample C is better dispersed and loaded on the surface of carbon after carbon coating, and the specific
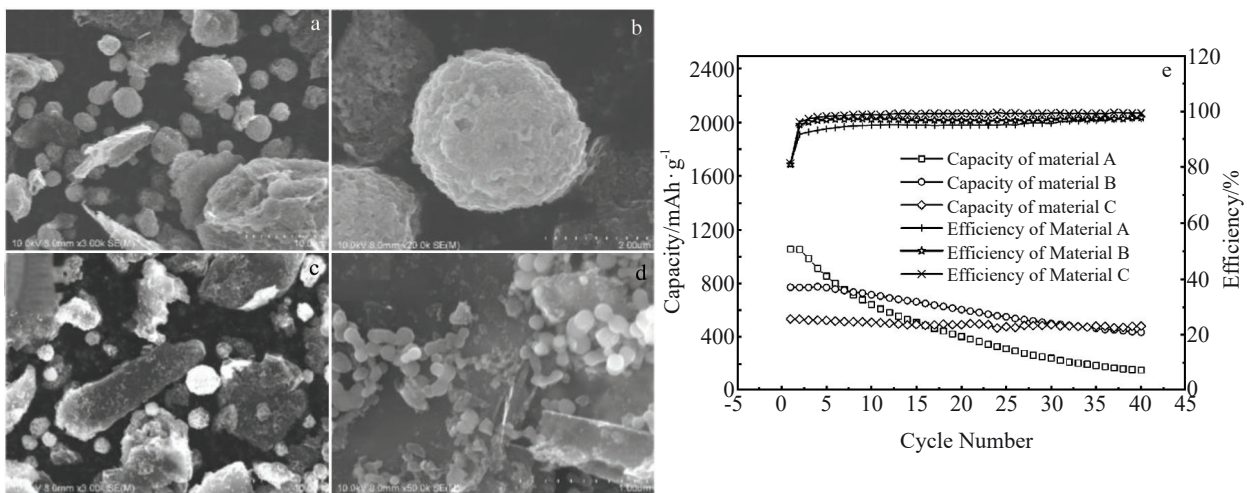

Fig.7　SEM images of the material A (a, b) and material B (c, d), and charge capacity and efficiency of Si/G/DC with different Si contents (e)

Table 1　Electrochemical properties of Si/G/DC with different Si contents

Cycle number	Sample A		Sample B		Sample C	
	Charge capacity/ mAh·g^{-1}	Efficiency/ %	Charge capacity/ mAh·g^{-1}	Capacity retention rate/%	Charge capacity/mAh·g^{-1}	Capacity retention rate/%
1st	1053	81.0	770	80.9	535	81.3
10th	641	60.9	715	92.8	509	95.1
20th	401	38.1	604	78.4	491	91.8

capacity of silicon for lithium removal is much higher than that of single nano-silicon.

Table 1 shows the electrochemical properties of Si/G/DC with different Si contents. Compared with sample B and C, the first charge capacity of sample A is increased by 36.8% and 96.8%, respectively, and the first charge capacity of sample B is increased by 43.9% compared with sample C, which is mainly due to the increase in silicon content. The first cycle efficiencies of sample A, B, C are 81.0%, 80.9% and 81.3%, respectively, which indicates that the first charge/discharge efficiencies of Si/G/C composites are mainly determined by carbon and have little relationship with silicon content. The 10th charge capacity of sample A, B, C is 641, 715 and 509 mAh/g, the 10th capacity retention rates are 60.9%, 92.8% and 95.1%, respectively; the 20th charge capacity is 401, 604 and 491 mAh/g, and the 20th capacity retention rates are 38.1%, 78.4% and 91.8%, respectively. Compared with sample C, the capacity of sample A at 10th is increased by 25.9%, and the capacity retention rate of sample A is decreased by 34.4% and 36.0% compared with sample B and C; the capacity of sample A at 20th is decreased by 33.6% and 18.1% compared with sample B and C, respectively. With the increase of the ratio of silicon to carbon, the number of agglomerated silicon spheres in the composites increases gradually, the agglomerations of silicon loaded on the surface of carbon particles become more serious, the damage to the electrode structure increases gradually, and the cycling performance of the materials decreases gradually. The ratio of silicon to carbon with sample C is a better choice for the preparation of composites used in this experiment.

3　Conclusions

1) An optimized Si/graphite/disordered-carbon (Si/G/DC) composite structure prepared by graphite, nano-silicon and amorphous carbon with thermal treatment of sucrose is proposed to improve the cycling performance.

2) With graphite as buffer matrix and conductive network and amorphous carbon coating, the Si/G/DC composite shows excellent electrochemical performance. The amorphous carbon coating in the Si/G/DC composite can apparently reduce the possibility of contact loss between silicon and electrolyte, and help to maintain the mechanical stability by relieving stresses resulting from silicon volume change.

References

1　Kasavajjula U, Wang C, Appleby A J. *Journal of Power Sources* [J], 2007, 163(2): 1003

2　Qi Peng, Chen Yungui, Zhu Ding *et al. Rare Metal Materials and Engineering*[J], 2014, 43(5): 1073

3　Nurpeissova A, Mukanova A, Kalimuldina G *et al. Nanomaterials*[J], 2020, 10(10): 1995

4　Wang H, Wei D, Wan Z *et al. Electrochimica Acta*[J], 2021, 368: 137 580

5　Marzari N, Ferretti A, Wolverton C. *Nature Materials*[J], 2021, 20(6): 736

6　Gu P, Rui C, Zhou Y *et al. Electrochimica Acta*[J], 2010, 55(12): 3876

7　Wang Wei, Kanchan Moni, Prashant Datta *et al. Journal of Materials Chemistry*[J], 2007, 30: 3229

8　He W, Li H, Long B *et al. ACS Applied Energy Materials*[J], 2021, 4(5): 4290

9　Luo Z, Xu Y, Gong C R *et al. Journal of Power Sources*[J], 2021, 485: 229 348

10　Zhu S, Lin Y, Yan Z *et al. Electrochimica Acta*[J], 2021, 377: 138 092

11　Wang Z, Zheng B, Liu H *et al. Journal of Alloys and Compounds*[J], 2021, 861: 157 955

12　Sui D, Xie Y, Zhao W *et al. Journal of Power Sources*[J], 2018, 384: 328

13　Zhang J, Zuo S, Wang Y *et al. Journal of Power Sources*[J], 2021, 495: 229 803

14　Padovano E, Giorcelli M, Bianchi G *et al. Journal of the European Ceramic Society*[J], 2019, 39(7): 2232

15　Ryu J, Bok T, Joo S H *et al. Energy Storage Materials*[J], 2021, 36: 139

16　Yu C, Tian X, Xiong Z *et al. Journal of Alloys and Compounds*[J], 2021, 869: 159 124

17　Zhou R, Guo H, Yang Y *et al. Alloys and Compounds*[J], 2016, 689: 130

18　Kim D P, Loka C, Joo S Y *et al. Materialia*[J], 2018, 4: 510

19　Li N, Liu Y, Ji X *et al. Chinese Chemical Letters*[J], 2021, 32: 3787

20　Li P, Kim H, Myung S T *et al. Energy Storage Materials*[J], 2021, 35: 550

21　Liu X Y, Zhao H W, Jiang S *et al. Journal of Alloys and Compounds*[J], 2021, 881: 160 442

22　Liang M W, Wang W J, Jiang Y *et al. Journal of Alloys and Compounds*[J], 2021, 878: 160 357

23　Qiu Y W, Zhang C Y, Zhang C K *et al. Journal of Alloys and*

Compounds[J], 2021, 877: 160 240

24 Liu D J, Han Z L, Ma J Q *et al. Chemical Engineering Journal* [J], 2021, 420: 129 754

25 Zhuo Y, Sun H, Uddin M H *et al. Electrochimica Acta*[J], 2021, 388: 138 522

26 Hu Y Y, You J H, Zhang S J *et al. Electrochimica Acta*[J], 2021, 386: 138 361

27 Zhang Y, Wang X Y, Ma L *et al. Powder Technology*[J], 2021, 388: 393

28 Chen Q J, Tan L, Wang S T *et al. Electrochimica Acta*[J], 2021,

385: 138 385

29 Jia H, Li X, Song J *et al. Nature Communications*[J], 2020, 11: 1474

30 Kalderon-Asael B, Katchinoff J A R, Planavsky N J *et al. Nature* [J], 2021, 595: 394

31 Hsu Y C, Hsieh C C, Liu W R *et al. Surface and Coatings Technology*[J], 2020, 387: 125 528

32 Ng S H, Wang J, Wexler D *et al. The Journal of Physical Chemistry C*[J], 2007, 111(29): 11 131

锂离子电池硅/石墨/无定形碳复合阳极材料的制备及电化学性能表征

李　涛[1,2]，李　蒙[2]，李　娜[1]，王长华[1]，朱冬霞[3]，张力久[1]，栗生辰[1]，邓　楠[1]

(1. 国标(北京)检验认证有限公司，北京 101400)

(2. 有研科技集团有限公司，北京 100088)

(3. 上海有色金属工业技术检测中心有限公司，上海 200431)

摘　要：提出并制备了一种优化结构的硅/石墨/无定形碳复合材料，材料主要通过对硅、石墨和蔗糖的混合物进行超细粉碎和热解制备，硅基材料的电化学性能得到有效改善。研究了硅/石墨/无定形碳材料的形貌、电化学性能、循环稳定性，并对硅含量进行了优化。结果表明，将纳米硅材料负载在石墨碳基体上，结合高温热解技术，可以有效提高阳极材料的电化学性能。以石墨为缓冲基体、具备导电网络和非晶碳涂层的硅/石墨/无定形碳材料表现出良好的电化学性能。硅/石墨/无定形碳材料的非晶碳涂层可以明显降低硅与电解液之间接触损耗的可能性，并通过释放硅体积变化产生的应力来帮助保持材料的稳定性。

关键词：锂离子电池；硅；硅/石墨/无定形碳复合材料；阳极

作者简介：李　涛，男，1980 年生，博士，正高级工程师，有研科技集团有限公司，北京 100088，电话：010-82241803，E-mail：ltao@grinm.com